Applied Surface Science 258 (2012) 7292–7298

Contents lists available at SciVerse ScienceDirect

Applied Surface Science

journal homepage: www.elsevier.com/locate/apsusc

On the surface characterization of an Al_2O_3 charge state conversion surface using ion scattering and atomic force microscope measurements

A. Riedo[a,*], M. Ruosch[b], M. Frenz[b], J.A. Scheer[a], P. Wurz[a]

[a] Physics Institute, Space Research and Planetary Sciences, Sidlerstrasse 5, 3012 Bern, Switzerland
[b] Institute of Applied Physics, Division of Biomedical Photonics, Sidlerstrasses 5, 3012 Bern, Switzerland

ARTICLE INFO

Article history:
Received 18 January 2012
Received in revised form 22 March 2012
Accepted 23 March 2012
Available online 3 April 2012

Keywords:
Ion scattering
AFM
Measurement sensitivity
Charge state conversion surface
Surface characterization
Space application

ABSTRACT

Thermal certification campaigns in the temperature ranges of −50 °C to +85 °C and −70 °C to +130 °C on charge state conversion surfaces (aluminum-oxide coatings on a silicon wafer substrate) were performed. Such surfaces are often used in neutral particle sensing instruments in space science where neutral atoms must be ionized prior to their analysis. Ion scattering and atomic force microscope (AFM) instruments were used to characterize the surface properties, e.g., surface roughness, angular scattering distribution and negative ionization efficiency of charge state conversion surfaces before and after thermal certification campaigns. No significant changes in surface roughness were found in AFM images whereas ion scattering measurements revealed a significant increase of the angular scattering distribution of up to 21% after thermal campaign in the expanded temperature range of −70 °C to +130 °C. The present study shows clearly that ion scattering measurements are sensitive enough to measure surface changes on atomic and sub atomic level whereas at this level the AFM instrument finds its limits.

1. Introduction

The interaction of atomic and molecular particles with charge state conversion surfaces has been researched extensively in recent years. Several types of conversion surfaces have been tested with regard to their scattering properties, their ability to convert neutral particles into ions (ionization efficiency) and their long-term stability, i.e., surface charging and damage [1–21]. Initial reports of relatively high ionization efficiencies of coated metal surfaces, e.g., Cesium on W(110) [11] or Barium on W(110) [12], made this technique attractive for space science and other applications. Further research showed that insulating surfaces suggested possibilities for several new applications because of their better long-term stability and ease of operation [1–10,13,14]. Among these applications, we use this ionization process in instruments on spacecraft for efficient detection of energetic neutral atoms originating in interplanetary or interstellar space in the energy range of 10 eV–2 keV [13,15,22]. This detection technique has already been successfully employed in several satellite missions, such as in the IMAGE (Imager for Magnetopause-to-Aurora Global Exploration) and the more recent IBEX (Interstellar Boundary EXplorer) satellite mission [9,10,23–25].

Natural diamond [15,16], diamond-like carbon (DLC) [14], MgO [13], $BaZrO_3$ [17], AlN [21] or LiF [8] conversion surfaces are only few examples of tested insulating surfaces, whereas natural diamond is currently the best candidate acting as conversion surface in neutral particle sensing instrumentation in space [10]. However, not only their surface properties are important factors but also their availability and price are crucial for an application in space science. Including these aspects, recent investigations have shown that DLC surfaces are good candidates to work as conversion surface in future space missions [10], which are used already in the IBEX-Lo instrument [26] on the IBEX mission [25]. Getting DLC coated surfaces in the required quality is, however, still difficult despite their widespread use in many other applications. Recent measurements have shown that Al_2O_3 coatings on silicon substrate charge state conversion surfaces are a possible alternative [18,19], and will be used in the BepiColombo space mission to Mercury, scheduled for launch in 2014. Silicon wafers are chosen because they are readily available and can be produced in large amounts with very low surface roughness. Silicon surfaces alone, without any coatings are due to their very low ionization efficiency of only some percent's for oxygen atoms with ion energies of few 100eV's not candidates for conversion surfaces [20].

The characterization of surface properties, e.g., surface roughness, surface charging, angular scattering distribution and the ability to convert neutral atoms to negatively charged ions (ionization efficiency), of charge state conversion surfaces is the most

* Corresponding author. Tel.: +41 316314449; fax: +41 316314405.
E-mail address: andreas.riedo@space.unibe.ch (A. Riedo).

0169-4332/$ – see front matter © 2012 Elsevier B.V. All rights reserved.
http://dx.doi.org/10.1016/j.apsusc.2012.03.139

important task to verify if a surface is suitable as conversion surface or not.

Electrical charging of the conversion surface can be by the primary ion beam (if applicable), by release of secondary electron emission by the incoming particle beam, and by photoelectron emission. Conversion surfaces with charging effects are not suitable candidates for neutral particle sensing instruments. The electric field of an electrically charged conversion surface can deflect outgoing ion trajectories and causing lower performance of the ion detection system, e.g., lower ion transmission and higher angular scattering distribution [18,19]. High ionization efficiencies and a low spread of angular scattering, which is correlated to low surface roughness [10,18,19], are the other two crucial parameters for a successful charge state conversion surface in a space instrument. The latter is important because a low spread of scattering angles minimizes scattered particle loss in downstream ion-optical analyzer systems and improves the imaging capabilities of the instrument. However, since the development of scanning tunneling microscopes (STM) and atomic force microscopes (AFM) in the 1980s, ion scattering measurements are used fewer and fewer to quantify surface properties even though ion scattering instruments are powerful tools that can directly provide angular scattering distributions and ionization efficiencies [27].

In this report thermal certification campaigns in the temperature ranges of −50 °C to +85 °C and −70 °C to +130 °C on aluminum-oxide on silicon substrate charge state conversion surfaces were performed. The conversion surfaces were characterized, regarding surface roughness, ionization efficiency and angular scattering, before and after thermal certification campaigns using an AFM and the Imager for Low Energetic Neutral Atoms (ILENA) ion scattering instrument. The certification campaigns are necessary to assure that these conversion surfaces operate in the expected thermal environment during the BepiColombo mission.

Scattering measurements were done at moderate vacuum conditions, i.e., in the low 10^{-7} mbar range, which mirrors the conditions within a typical particle sensing instrument on a satellite shortly after launch [28–30]. Molecular oxygen and atomic neon ion beams in the ion energy range of 390 eV up to 1000 eV were used to investigate the surfaces. At ion energies of up to 1000 eV the incidence ion dose on the sample can be estimated to about 10^7 ions/cm^2 s, corresponding to an ion current in the low pA range. A monolayer on a surface contains about 10^{15} atoms/cm^2. Therefore, no surface damage due to the incoming beam is expected. The penetration depth of the ions at these conditions, e.g., low ion energy and shallow incidence of the ions relative to the surface of 8°, is estimated to be three monolayers at maximum [31].

2. Experiment

The surfaces investigated were amorphous aluminum-oxide (Al_2O_3) coatings of 25 nm thickness on silicon single crystal substrate charge state conversion surfaces (Thin Film Physics, Switzerland). The silicon single-crystal substrates (randomly orientated, doping level as low as possible) were cleaned in different ultrasonic baths and finally plasma cleaned prior the deposition of the coating. The coatings were produced at a coating temperature of 100 °C, under high vacuum conditions and using the plasma vapor deposition method. Thin coatings on silicon substrates were chosen because previous performance studies on aluminum-oxide single crystals showed surface charging effects whereas thin alumina films on silicon substrates did not [18,19]. If a low charge effect is still present the influences on the ion beam are below the detection sensitivity of the instrument. The thinnest coating, of 25 nm thickness, showed the best performance for our application [19]. The conversion surfaces discussed in this study will be

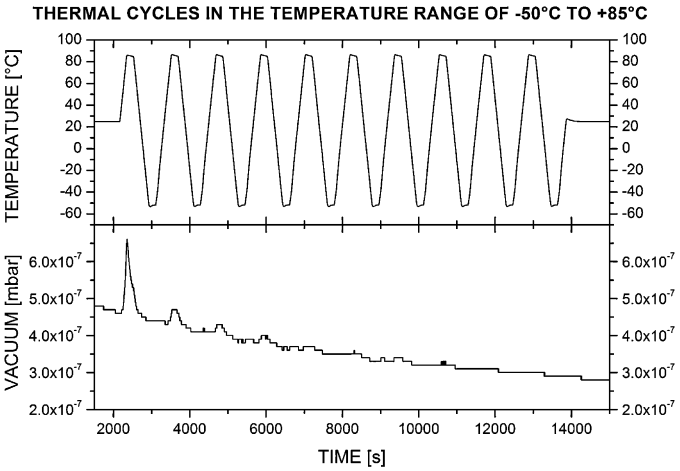

Fig. 1. Top panel: Actual measurement of the temperature during the thermal cycles in the temperature range of −50 °C to +85 °C. Bottom panel: Vacuum pressure during the thermal cycles. The first strong peak corresponds to the first heating cycle and is correlated mainly to residual water desorbed from the surface, which outgases more efficiently at increased temperatures.

used in the Energetic Neutral Atoms (ENA) instrument on board the space mission BepiColombo for the detailed investigation of the planet Mercury. More information on the conversion surfaces and the BepiColombo mission can be found in [18,19,30,32,33].

Two thermal certification campaigns with different temperature ranges were performed based on the expected thermal environment during the BepiColombo mission. The first campaign was conducted for the nominal temperature range of −50 °C to +85 °C (i.e., over a temperature range of ΔT = 135 °C) of the ENA instrument and the second campaign for an expanded temperature range of −70 °C to +130 °C (ΔT = 200 °C). In each campaign 10 thermal cycles in the given temperature ranges were performed (see Figs. 1 and 2). The temperature cycles were performed in vacuum, in the MEFISTO facility [34,35], of the Physics Institute, on a heating/cooling plate. The base pressure in the MEFISTO chamber was herby in the mid 10^{-7} mbar range to assure to have no temperature exchange via convection (see Figs. 1 and 2). In both campaigns new and identical charge state conversion surfaces were used. Each surface was investigated, regarding surface roughness,

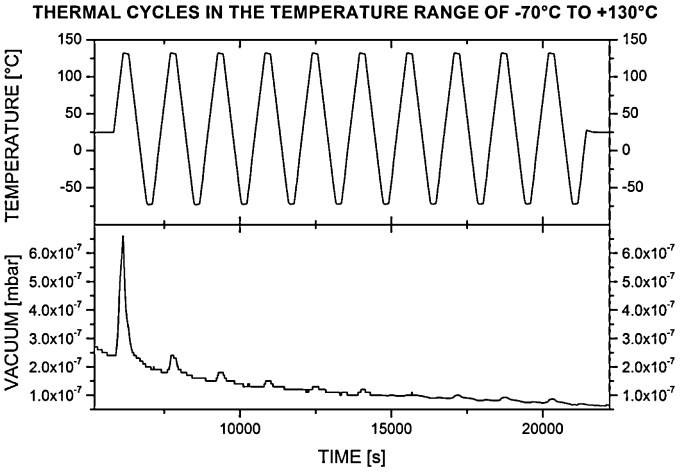

Fig. 2. Top panel: Actual measurement of the temperature during the thermal cycles in the temperature range of −70 °C to +130 °C. Bottom panel: Vacuum pressure during the thermal cycles. The first strong peak corresponds to the first heating cycle and is correlated mainly to residual water desorbed from the surface, which outgases more efficiently at increased temperatures.

ionization efficiency and angular scattering, before and after the thermal campaigns using ion scattering and AFM measurements.

Surface scattering measurements were done with the Imager for low energetic neutral atoms (ILENA), of the Physics Institute, and an AFM, Institute of Applied Physics. Further details on the experimental setups and measurement procedure can be found in the next two subsections.

2.1. AFM

Measurements on surface roughness were done using an AFM (Bioscope II, Veeco, Germany) before and after the thermal certification campaigns. Sharp Nitride Lever probes with nominal spring constant of 0.12 N/m and nominal tip radius of 2 nm were used for this study. All measurements were made in contact mode with a contact force of about 11 nN on different positions on each charge state conversion surface at ambient pressure and temperature. No additional liquids were used for the AFM measurements. In each measurement an area of $1 \times 1\ \mu m$ was investigated, with a spatial resolution of 2048×2048 pixels. The quoted measurement uncertainty of the surface roughness is 1.0 Å RMS, given by instrument specifications (bioscope ii manual-g (004-991-000).pdf, p. 51), only if all acoustic and vibration specifications are fulfilled.

To verify the proper function of the AFM a DLC conversion surface (tetrahedral amorphous-carbon (ta-C) films on silicon single crystal substrates) with a known surface roughness was used. The surface roughness of the DLC conversion surface was given from the manufacturer and is max. 4.5 Å RMS, the measurement uncertainty is unknown. With the AFM instrument we measured on 5 different surface locations a mean surface roughness of (3.3 ± 1.0) Å, which is slightly lower than the surface roughness given from the manufacturer. Detailed information about this conversion surface can be found in [10,30].

2.2. ILENA – Imager for low energetic neutral atoms

Particle scattering measurements were made with the imager for low energetic neutral atoms (ILENA) apparatus at the Space Research and Planetary Sciences division, University of Bern, Switzerland. Fig. 3 displays an overview of the ILENA experimental setup. The energy range of incident particles, e.g., Ne and molecular oxygen O_2, chosen for these measurements was 390–1000 eV. For all measurements the angle of incidence was 8° with respect to the surface normal. The full angular scattering distribution was recorded by rotating the imaging detector to the optimal position of the scattered peak. The experimental setup is described in brief below; further in details are given in [15,21,36].

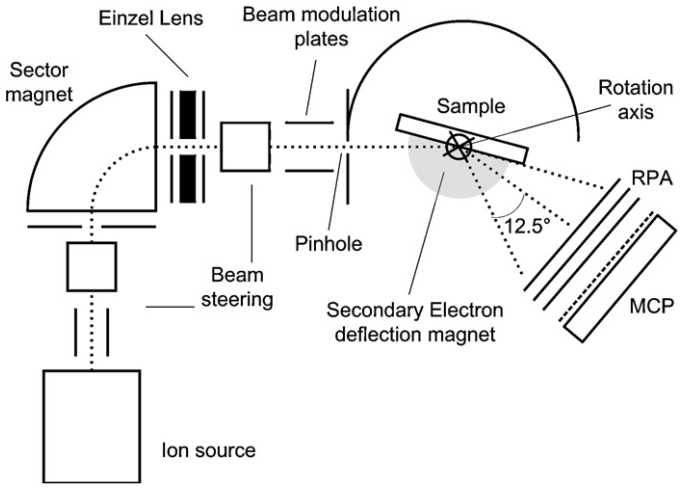

Fig. 3. Schematic overview of the ILENA experiment.

The ILENA apparatus consists of an ion source, a magnetic ion separator providing a mass resolution of $m/\Delta m \approx 45$, an ion beam guiding system, a sample stage with housing and a detection unit. All these units are contained in a single vacuum chamber pumped by an ion getter pump. The reflected beam is recorded using a two-dimensional position-sensitive MCP detector with a viewing angle of ±12.5° in both, azimuthal and polar directions.

After passing the pinhole the ion beam has a beam diameter of 1 mm. Hence, ion scattering measurements represents an averaged measurement over a conversion surface area of about 0.8 mm^2. A typical measurement of the angular scatter distribution is shown in Fig. 4. The direction of angular deviation from specular scattering that resides in a plane containing the incoming trajectory and normal to the surface is defined as polar scattering. The direction of specular scattering normal to the polar angle plane is defined as azimuthal scattering, with zero indicating a true specular reflection (see Fig. 4). The angular scattering in polar and azimuthal direction can be measured with the measurement uncertainties of ±0.5 and ±1.0 degrees, respectively.

A retarding potential analyzer (RPA) consisting of three grids is mounted in front of the MCP detector. The detector unit, including the RPA, is shielded electrostatically and can be rotated independently from the converter surface around the same axis. The outer grids of the RPA are grounded to shield the inner grid, which can be biased to suppress ions. An additional grid in front of the MCP detector at negative potential with respect to the MCP detector serves to reject secondary electrons originating from the preceding grids

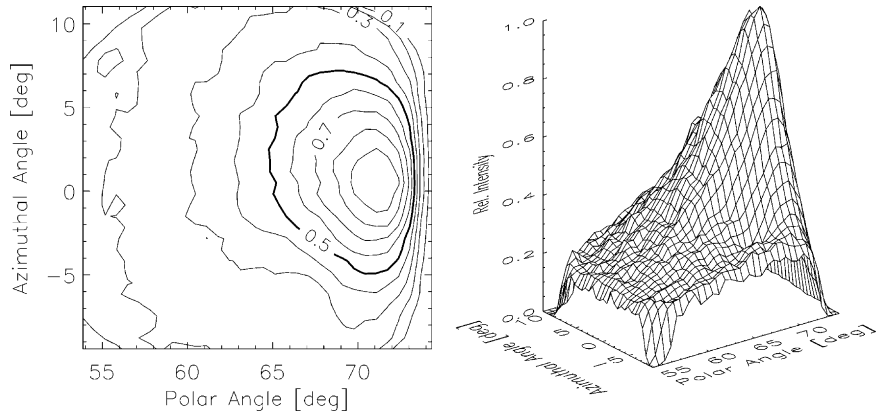

Fig. 4. Left: Contour plot of the angular scattering distribution of a 390 eV O_2^+ ion beam scattered on the Al_2O_3/Si charge state conversion surface before thermal cycles were performed. The bold line indicates the 50% level (FWHM) of the detected peak. Right: Same data displayed in three dimensions.

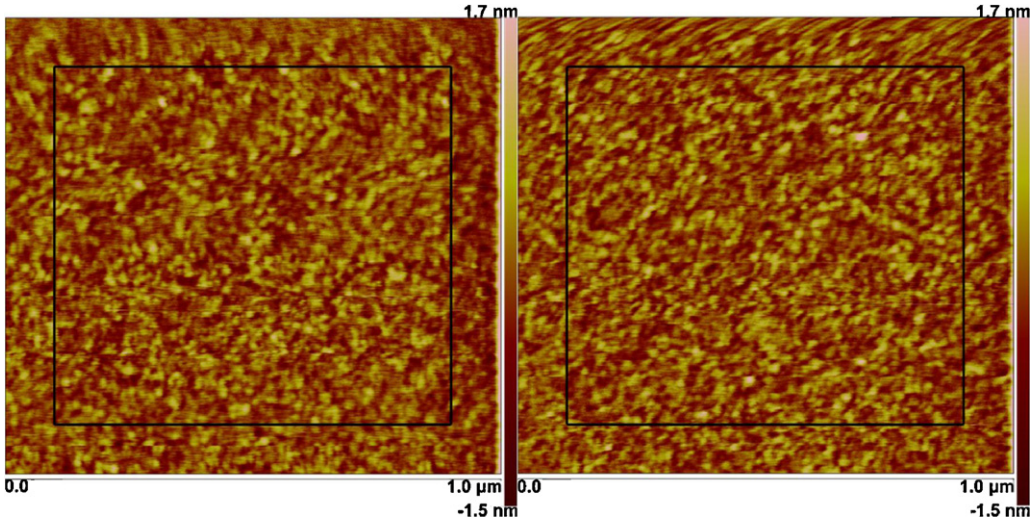

Fig. 5. Typical AFM images before (left) and after (right) the thermal certification campaign in the temperature range of −50 °C to +85 °C on the Al_2O_3/Si charge state conversion surfaces. No significant increase of the surface roughness due to the thermal stress was measured.

and the conversion surface. The MCP detector may be floated at a high negative voltage to vary the transmission threshold for negative particles. After baking out the vacuum chamber at +80 °C for several hours, a residual gas pressure in the mid 10^{-8} mbar range is achieved. During operation the pressure may rise into the low 10^{-7} mbar range as a result of test gas, Ne and O_2, leaking into the ion source chamber.

The fraction of negative ions was determined by taking measurements with and without an applied floating voltage on the MCP detector. In the first case, only neutral particles were recorded, in the latter case neutral particles and negative ions were recorded simultaneously. The difference gives the fraction of negative ions. Each data-point results from a series of successive measurements, which allows the registration of ion beam drifts and possible surface charging during each measurement series. With the MCP detector it was not possible to distinguish between scattered and negatively ionized primary oxygen particles and sputtered negative ions from the conversion surface. Therefore, neon without the ability to form negative ions and with a comparable mass to oxygen was taken as a proxy to assess the background of sputtered negative ions for the evaluation of the negative ionization yield of molecular oxygen. The sputtered fractions were finally subtracted from the negative ionization yields of oxygen. Oxygen and neon were chosen because they allow for a sensitive and reliable measurement of deteriorating effects, e.g., ionization efficiency and angular scattering, on the conversion surface. The detection efficiency of the MCP is taken from [37,38] where an identical detector was used.

3. Results

3.1. AFM measurements

Fig. 5 shows typical AFM images taken before and after the thermal campaign in the temperature range of −50 °C to +85 °C. Within the estimated measurement uncertainties of ±1.0 Å no significant changes in surface roughness due to the thermal stress were measured. The mean surface roughness measured before and after the thermal cycles was $R_{RMS,before} = (3.4 \pm 1.0)$ Å and $R_{RMS,after} = (3.4 \pm 1.0)$ Å. All measurements are listed in Table 1. Furthermore, no significant increase in surface roughness before and after the second, the expanded thermal range campaign (i.e., in the

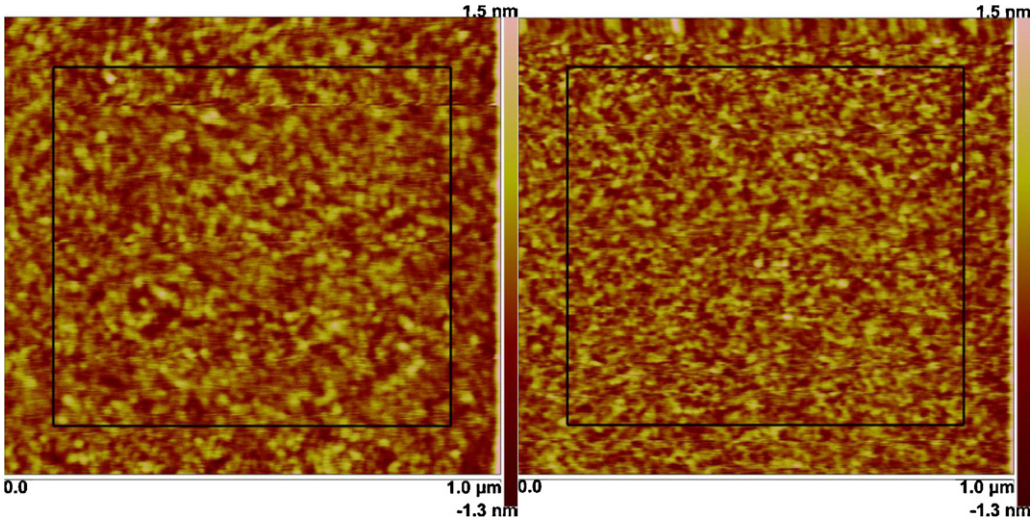

Fig. 6. Typical AFM images before (left) and after (right) the thermal certification campaign in the temperature range of −70 °C to +130 °C on the Al_2O_3/Si charge state conversion surfaces. No significant increase of the surface roughness due to the thermal stress was measured.

Table 1
Surface roughness measured with the AFM before (left column) and after (right column) thermal certification campaign in the temperature range of −50 °C to +85 °C. Measurements were performed at three locations on the surface.

$R_{b1} = (3.3 \pm 1.0)$ Å	$R_{a1} = (3.4 \pm 1.0)$ Å
$R_{b2} = (3.4 \pm 1.0)$ Å	$R_{a2} = (3.2 \pm 1.0)$ Å
$R_{b3} = (3.4 \pm 1.0)$ Å	$R_{a3} = (3.5 \pm 1.0)$ Å
$R_{b,mean} = (3.4 \pm 1.0)$ Å	$R_{a,mean} = (3.4 \pm 1.0)$ Å

temperature range of −70 °C to +130 °C, see Fig. 6), was observed. The measured roughness before and after the thermal cycles was found to be $R_{RMS,before} = (2.7 \pm 1.0)$ Å and $R_{RMS,after} = (3.1 \pm 1.0)$ Å, respectively. These measurements are listed in Table 2.

3.2. Ion scattering measurements

Fig. 7 shows the ion scattering measurement results before and after the first thermal certification campaign in the temperature range of −50 °C to +85 °C. Within the measurement uncertainties no significant changes in negative ionization efficiency nor in the angular scattering distribution, polar and azimuthal, were found.

Fig. 8 shows the measurements before and after the thermal cycles for the enlarged temperature range of −70 °C to +130 °C. Again, within the measurement uncertainties no significant changes in the ionization efficiency were found. However, and in contrast to the measurement results of the first thermal campaign, significant changes in both the polar and azimuthal angular scattering directions were found. Changes in angular scattering in polar direction of up to 17% and 21% were found for neon and molecular oxygen ions, respectively, at the highest ion energy of 1000 eV. Even for the lowest ion energy of 390 eV changes in angular scattering in polar direction of molecular oxygen and neon were observed. In azimuthal direction changes of up to 15% and 19% for neon and molecular oxygen ions, respectively, at ion energy 1000 eV were measured.

4. Discussion

Regarding the thermal certification campaign in the lower temperature range of −50 °C to +85 °C, no differences in surface properties, e.g., surface roughness, ionization efficiency and angular scattering distribution, before and after the thermal campaign using AFM and ion scattering measurements were found (see Figs. 5 and 7, Table 1). Both, the ion scattering experiment and AFM images give the same measurement result, i.e., no change in surface properties. This is, however, different in the expanded thermal certification campaign in the temperature range of −70 °C to +130 °C (see Figs. 6 and 8, Table 2). Ion scattering measurements clearly revealed a significant increase of angular scattering of up to 21% (O_2 at 1000 eV in polar direction), i.e., an increase in the average surface roughness on atomic level. Similar findings concerning increased angular scattering distribution with increased surface roughness are reported in [10,18,19,39] where different conversion surface, i.e., DLC (Sandia National Laboratories, USA), amorphous carbon, Al_2O_3 conversion surfaces etc., with different surface roughness were investigated. A detailed discussion on ion particle-surface interactions, theoretical models and simulations can be found in the reports [7,39]. However, in contrast to the scattering measurements, the AFM images showed no increase of surface roughness within the estimated measurement uncertainties.

Table 2
Surface roughness measured with AFM before (left column) and after (right column) thermal certification campaign in the temperature range of −70 °C to +135 °C. Three measurements on different surface locations were done before thermal campaign. Because previous measurements showed high measurement reproducibility, only two instead of three measurements on different surface locations after the campaign were performed.

$R_{b1} = (2.8 \pm 1.0)$ Å	$R_{a1} = (3.2 \pm 1.0)$ Å
$R_{b2} = (2.7 \pm 1.0)$ Å	$R_{a2} = (3.0 \pm 1.0)$ Å
$R_{b3} = (2.7 \pm 1.0)$ Å	
$R_{b,mean} = (2.7 \pm 1.0)$ Å	$R_{a,mean} = (3.1 \pm 1.0)$ Å

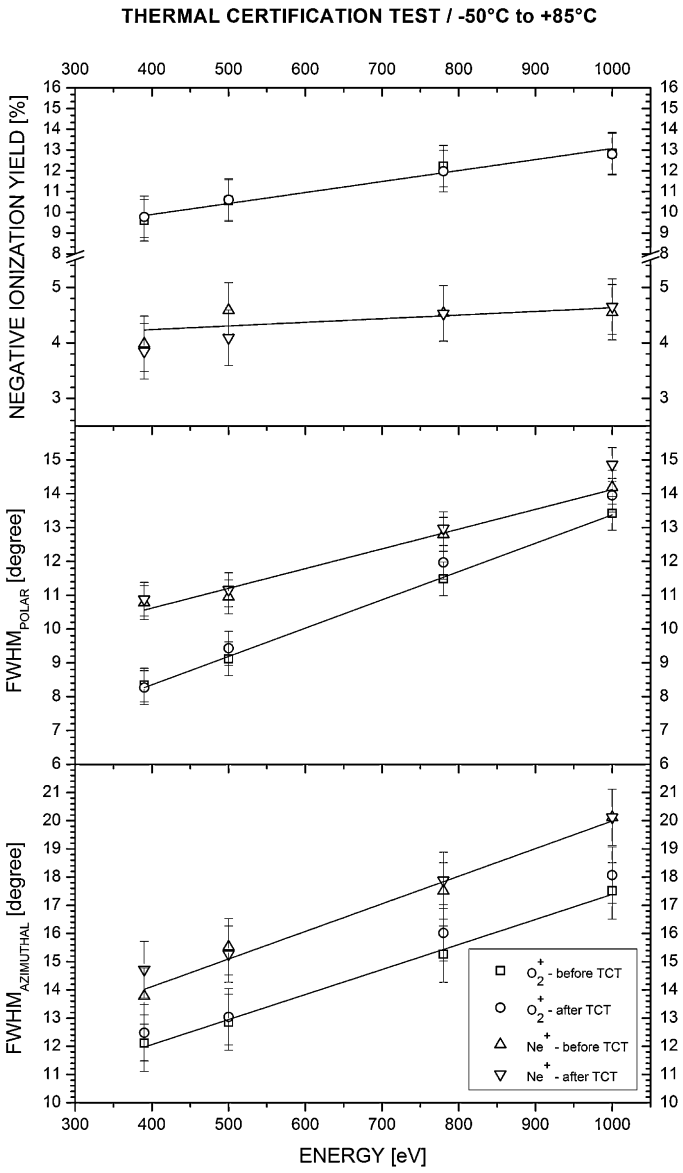

Fig. 7. Ion scattering measurements done before and after the first thermal certification campaign in the temperature range of −50 °C to +85 °C are displayed. Top panel: Negative ionization yield. Middle and bottom panel: Angular scattering distribution in polar and azimuthal direction. No significant changes were found in the ionization yield and angular scattering measured before and after the thermal cycle. The lines are linear regressions of the measurements done before the thermal cycles and are given to guide the eye.

Changes in surface properties, e.g., angular scattering distribution, in the expanded temperature range of −70 °C to +130 °C were measured (see Fig. 8). The silicon single crystal substrate of the charge state conversion surface was coated with Al_2O_3 (25 nm) at a coating temperature of 100 °C. Thus, the thermal certification campaign in the temperature range of −50 °C to +85 °C (ΔT = 135 °C) does not exceed the coating temperature of 100 °C. This is different in the expanded temperature campaign. The thermal certification campaign in the temperature range of −70 °C to +130 °C (ΔT = 200 °C) exceeded the coating temperature by 30 °C.

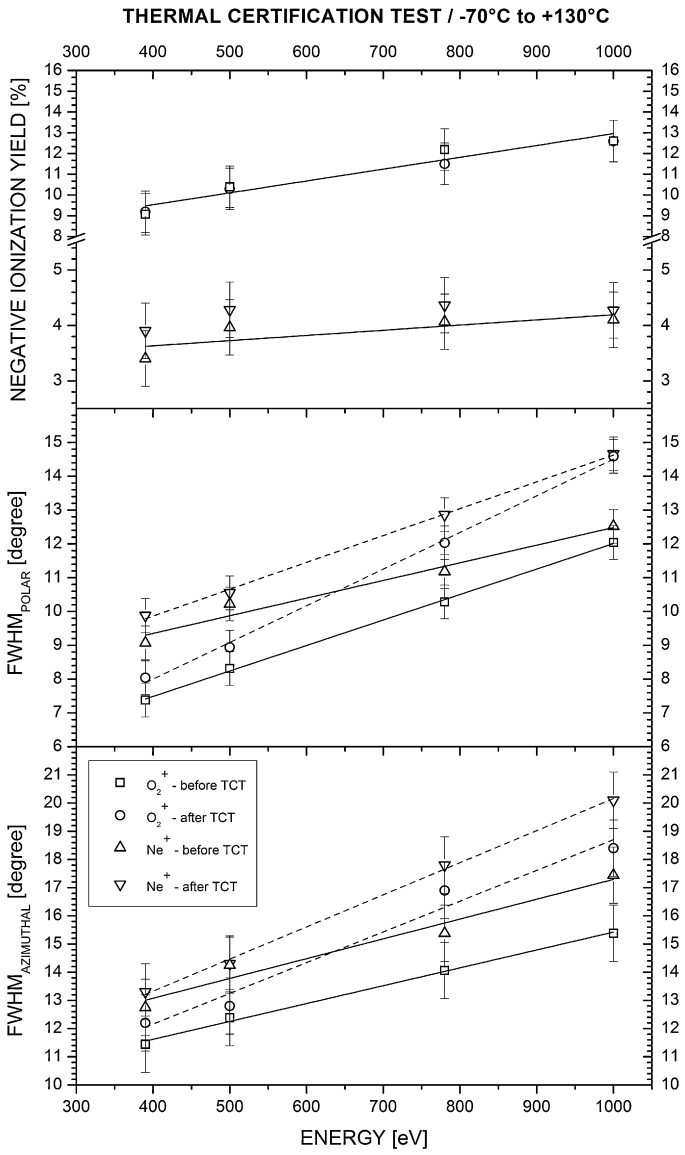

Fig. 8. Ion scattering measurement done before and after the first thermal certification campaign in the temperature range of −70 °C to +130 °C are displayed. Top panel: Negative ionization yield, where no significant changes were measured within the measurement uncertainties. Middle and bottom panel: Angular scattering distribution in polar and azimuthal direction. Significant changes at higher ion energies, e.g. 780 eV and 1000 eV, are clearly visible. Changes of up to 21% for molecular oxygen ions at ion energy of 1000 eV in polar direction were measured. Full and dashed lines are linear regressions of the measurements done before, after respectively the thermal cycles and are given to guide the eye.

Apparently, temperatures exceeding the coating temperature of 100 °C can cause a degradation of the charge state conversions surface and hence changes in surface properties, e.g., surface roughness, etc.

A general trend of increasing angular scattering with increasing incident energy was measured (Figs. 7 and 8). This trend can be understood because higher particle energies probe the surface potential at deeper levels where the corrugation of the surface potential is larger, resulting in a larger angular scattering distribution. In Figs. 7 and 8 increasing ionization efficiencies with increasing energy of the incident ions can be seen. Similar findings have been reported for other insulating surfaces like LiF [8], MgO [13] and $BaZrO_3$ [17], and we agree with the interpretation that higher energies cause smaller distances of closest approach between scattered ions and surface atoms, which results in higher probabilities for the charge exchange processes and thus yield higher fractions of negative ions.

It still has to be explained how charge exchange happens when particles scatter off an insulating surface. According to [40] and [41], the width of the band gap of Al_2O_3 is about 9 eV. The negative electron affinity level of O is 1.46 eV below the vacuum level. The valence band is filled and there is no electron mobility in an insulator. So, one should not expect that charge exchange would be possible. But it has been found that for ionic crystals such as, for instance, LiF, charge exchange proceeds via capture of electrons from the anionic sites of the surface in a binary ion–atom interaction [42–44]. Once the negative ion is formed it cannot be neutralized by resonant electron loss to the solid, as in the case of metals, because of the band gap of the ionic crystal. It is safe to expect a similar behavior here. In addition, the probability for a particle to be negatively charged increases with increasing effective number of collisions, and thus at grazing incidence angles.

5. Conclusion

Thermal certification campaigns in the temperature ranges of −50 °C to +85 °C and −70 °C to +130 °C on charge state conversion surfaces were done. AFM at ambient pressure and ion scattering measurements were used to characterize surface properties, e.g., surface roughness, ionization efficiency and angular scattering distribution, before and after each thermal campaign. No significant changes in surface properties were found in AFM and ion scattering measurements after the thermal campaign in the temperature range of −50 °C to +85 °C. In the expanded temperature range of −70 °C to +130 °C ion scattering measurement showed clearly changes on atomic and sub atomic level as a result of a significant increase in angular scattering, whereas AFM images showed no significant changes in surface roughness. We can conclude that ion scattering experiments are a powerful tool to characterize surface properties, e.g., ionization efficiency and angular scattering distribution, which depends on surface roughness. Because ions are used to probe the surface, ion scattering instruments measure changes on atomic and sub atomic level and can be regarded as a comparable and alternative tool to AFM for this kind of investigations.

Acknowledgment

This work is supported by the Swiss National Science Foundation.

References

[1] C. Auth, A.G. Borisov, H. Winter, High fractions of negative ions in grazing scattering of fast oxygen atoms from a LiF(100) surface, Phys. Rev. Lett. 75 (1995) 2292–2295.
[2] P. Stracke, F. Wiegershaus, S. Krischok, H. Müller, V. Kempter, Electron emission from temporary negative $N^{-*}(^1D)$ ions formed in slow collisions of N^+ with insulator surfaces (LiF; CsI), Nucl. Instrum. Methods Phys. Res. B 125 (1997) 63–66.
[3] S.A. Deutscher, A.G. Borisov, V. Sidis, Formation of negative ions from fluorine projectiles scattered off a MgO(100) surface: theory, Phys. Rev. A 59 (1999) 4446–4455.
[4] P. Roncin, J. Villette, J.P. Atanas, H. Khemliche, Energy loss of low energy protons on LiF(100): surface excitation and H^- mediated electron emission, Phys. Rev. Lett. 83 (1999) 864–867.
[5] A.G. Borisov, V.A. Esaulov, Negative ion formation in the scattering of atoms and ions from dielectric surfaces, J. Phys.: Condens. Matter 12 (2000) R177.
[6] R. Souda, Femtosecond electron dynamics on solid surfaces probed by ion scattering and stimulated desorption of secondary ions, Int. J. Mod. Phys. B 14 (2000) 1139–1177.
[7] H. Winter, Collisions of atoms and ions with surfaces under grazing incidence, Phys. Rep. 367 (2002) 387–582.
[8] J.A. Scheer, P. Wurz, W. Heiland, Scattering of slow ions from insulator surfaces at the example of molecular oxygen from LiF(100), Nucl. Instrum. Methods Phys. Res. B 212 (2003) 291–296.

[9] J.A. Scheer, M. Wieser, P. Wurz, P. Bochsler, E. Hertzberg, S.A. Fuselier, F.A. Koeck, R.J. Nemanich, M. Schleberger, High negative ion yield from light molecule scattering, Nucl. Instrum. Methods Phys. Res. B 230 (2005) 330–339.
[10] J.A. Scheer, M. Wieser, P. Wurz, P. Bochsler, E. Hertzberg, S.A. Fuselier, F.A. Koeck, R.J. Nemanich, M. Schleberger, Conversion surfaces for neutral particle imaging detectors, Adv. Space Res. 38 (2006) 664–671.
[11] M.R. Aellig, P. Wurz, R. Schletti, P. Bochsler, A.G. Ghielmetti, E.G. Shelley, S.A. Fuselier, J. Quinn, F. Herrero, M.F. Smith, Surface ionization with cesiated converters for space applications, American Geophysical Union Monograph on Measurement Techniques for Space Plasmas, vol. 103, 1998, pp. 289–294.
[12] R. Schletti, Master Thesis, Anwendung der Oberflächenionisation in Raumforschungsexperimenten, University of Bern, Switzerland, 1996.
[13] M. Wieser, P. Wurz, K. Brüning, W. Heiland, Scattering of atoms and molecules off a magnesium oxide surface, Nucl. Instrum. Methods Phys. Res. B 192 (2002) 370–380.
[14] J. Scheer, M. Wieser, P. Wurz, P. Bochsler, E. Hertzberg, S.A. Fuselier, F.A. Koeck, R.J. Nemanich, M. Schleberger, High negative ion yield from light molecule scattering, Nucl. Instrum. Methods Phys. Res. B 230 (2005) 330–339.
[15] P. Wurz, R. Schletti, M.R. Aellig, Hydrogen and oxygen negative ion production by surface ionization using diamond surfaces, Surf. Sci. 373 (1997) 56–66.
[16] J. Scheer, K. Brünnig, T. Fröhlich, P. Wurz, W. Heiland, Scattering of small molecules from a diamond surface, Nucl. Instrum. Methods Phys. Res. B 157 (1999) 208–213.
[17] S. Jans, P. Wurz, R. Schletti, K. Brünnig, K. Sekar, W. Heiland, J. Quinn, R.E. Leuchtner, Scattering of atoms and molecules off a barium zirconate surface, Nucl. Instrum. Methods Phys. Res. B 173 (2001) 503–515.
[18] J.A. Scheer, P. Wahlström, P. Wurz, Scattering of light molecules from Al_2O_3 surfaces, Nucl. Instrum. Methods B 256 (2007) 76–80.
[19] J.A. Scheer, P. Wahlström, P. Wurz, Scattering of light molecules from thin Al_2O_3 films, Nucl. Instrum. Methods B 267 (2009) 2571–2574.
[20] M. Shappirio, M. Coplan, E. Balsamo, D. Chornay, M. Collier, P. Hughes, J. Keller, K. Ogilvie, American Geophysical Union, Fall Meeting 2008, abstract #SM41B-1684.
[21] S. Jans, P. Wurz, R. Schletti, T. Fröhlich, E. Hertzberg, S. Fuselier, Negative ion production by surface ionization at aluminum-nitride surfaces, J. Appl. Phys. 87 (2000) 2587–2592.
[22] P. Wurz, The Outer Heliosphere: Beyond the Planets, Copernikus Gesellschaft e.V., Katlenburg-Lindau, 2000, p. 251.
[23] T.E. Moore, D.J. Chornay, M.R. Collier, F.A. Herrero, J. Johnson, M.A. Johnson, J.W. Keller, J.F. Laudadio, J.F. Lobell, K.W. Ogilvie, P. Rozmarynowski, S.A. Fuselier, A.G. Ghielmetti, E. Hertzberg, D.C. Hamilton, R. Lundgren, P. Wilson, P. Walpole, T.M. Stephen, B.L. Peko, B. van Zyl, P. Wurz, J.M. Quinn, G.R. Wilson, The low-energy neutral atom imager for IMAGE, Space Sci. Rev. 91 (2000) 155–195.
[24] P. Wurz, M.R. Aellig, P. Bochsler, A.G. Ghielmetti, E.G. Shelley, S. Fuselier, F. Herrero, M.F. Smith, T. Stephen, Neutral atom imaging mass spectrograph, Opt. Eng. 34 (1995) 2365–2376.
[25] D.J. McComas, F. Allegrini, P. Bochsler, M. Bzowski, M. Collier, H. Fahr, H. Fichtner, P. Frisch, H.O. Funsten, S.A. Fuselier, G. Gloeckler, M. Gruntman, V. Izmodenov, P. Knappenberger, M. Lee, S. Livi, D. Mitchell, E. Möbius, T. Moore, S. Pope, D. Reisenfeld, E. Roelof, J. Scherrer, N. Schwadron, R. Tyler, M. Wieser, M. Witte, P. Wurz, G. Zank, IBEX – The Interstellar Boundary Explorer, Space Sci. Rev. 146 (2009) 11–33.
[26] S.A. Fuselier, P. Bochsler, D. Chornay, G. Clark, G.B. Crew, G. Dunn, S. Ellis, T. Friedmann, H.O. Funsten, A.G. Ghielmetti, J. Googins, M.S. Grano, J.W. Hamilton, J. Hanley, D. Heirtzler, E. Hertzberg, D. Isaac, B. King, U. Knauss, H. Kucharek, F. Kudirka, S. Livi, J. Lobell, S. Longworth, K. Mashburn, D.J. McComas, E. Möbius, A.S. Moore, T.E. Moore, R.J. Nemanich, J. Nolin, M. O'Neal, D. Piazza, L. Peterson, S.E. Pope, P. Rosmarynowski, L.A. Saul, J.R. Scherrer, J.A. Scheer, C. Schlemm, N.A. Schwadron, C. Tillier, S. Turco, J. Tyler, M. Vosbury, M. Wieser, P. Wurz, S. Zaffke, The IBEX-Lo Sensor, Space Sci. Rev. 146 (2009) 117–147.
[27] G. Binnig, C.F. Quate, Ch. Gerber, Atomic force microscope, Phys. Rev. Lett. 56 (1986) 930–933.
[28] B. Schläppi, K. Altwegg, H. Balsiger, M. Hässig, A. Jäckel, P. Wurz, B. Fiethe, M. Rubin, S.A. Fuselier, J.-J. Berthelier, J. De Keyser, H. Rème, U. Mall, The influence of spacecraft outgassing on the exploration of tenuous atmospheres with in situ mass spectrometry, J. Geophys. 115 (2010) A12313.
[29] S. Graf, K. Altwegg, H. Balsiger, P. Bochsler, B. Fiethe, E. Montagnon, Thruster plumes: sources for high pressure and contamination at the payload location, J. Spacecraft Rockets 45 (2008) 57–64.
[30] A. Riedo, P. Wahlström, J.A. Scheer, P. Wurz, M. Tulej, Effect of long duration UV irradiation on diamondlike carbon surfaces in the presence of a hydrocarbon gaseous atmosphere, J. Appl. Phys. 108 (2010) 114915.
[31] A. Närmann, W. Heiland, R. Monreal, F. Flores, P.M. Echenqiue, Charge exchange and energy loss of particles interaction with surfaces, Phys. Rev. B 44 (1991) 2003–2018.
[32] Y. Saito, J.A. Sauvaud, M. Hirahara, S. Barabash, D. Delcourt, T. Takashima, K. Asamura, BepiColombo MMO/MPPE Team, Scientific objectives and instrumentation of Mercury Plasma Particle Experiment (MPPE) onboard MMO, Planet. Space Sci. 58 (2010) 182–200.
[33] J. Benkhoff, J. van Casteren, H. Hayakawa, M. Fujimoto, H. Laakso, M. Novara, P. Ferri, H.R. Middleton, R. Ziethe, BepiColombo – Comprehensive exploration of mercury: mission overview and science goals, Planet. Space Sci. 58 (2010) 2–20.
[34] A. Marti, R. Schletti, P. Wurz, P. Bochsler, Calibration facility for solar wind plasma instrumentation, Rev. Sci. Instrum. 72 (2001) 1354–1360.
[35] P. Wurz, A. Marti, P. Bochsler, New test facility for solar wind instrumentation, in: J. Schacher (Ed.), Proceedings of the Spring Meeting of the Swiss Physical Society, Helv. Phys. Acta 71 (Separanda 1) (1998) 23–24.
[36] P. Wahlström, J.A. Scheer, A. Riedo, P. Wurz, M. Wieser, Test facility to study surface interaction processes for particle detection in space, J. Spacecraft Rockets, submitted for publication.
[37] B.L. Peko, T.M. Stephen, Absolute detection efficiencies of low energy H, H^-, H^+, H_2^+ and H_3^+ incident on a multichannel plate detector, Nucl. Instrum. Methods B 171 (2000) 597–604.
[38] T.M. Stephen, B.L. Peko, Absolute calibration of a multichannel plate detector for low energy O, O^-, and O^+, Rev. Sci. Instrum. 71 (2000) 1355–1359.
[39] H. Niehus, W. Heiland, E. Taglauer, Low-energy ion scattering at surfaces, Surf. Sci. Rep. 17 (1993) 213–303.
[40] I. Batra, Electronic structure of α-Al_2O_3, J. Phys. C: Solid State Phys. 15 (1982) 5399–5410.
[41] V.M. Fomin, V.R. Misko, J.T. Devreese, H.H. Brongersma, Comparative analysis of the low-energy He^+ ions scattering on Al and Al_2O_3 surfaces, Nucl. Instrum. Methods Phys. Res. B 145 (1998) 545–552.
[42] C. Auth, A. Mertens, H. Winter, A.G. Borisov, V. Sidis, Formation of negative ions in grazing scattering from insulator surfaces, Phys. Rev. A 57 (1998) 351–361.
[43] F.W. Meyer, Q. Yan, P. Zeijlmans van Emmichoven, I.G. Hughes, G. Spierings, On the neutralization of singly and multicharged projectiles during grazing interactions with LiF(100), Nucl. Instrum. Methods Phys. Res. B 125 (1997) 138–145.
[44] S. Ustaze, R. Verrucchi, S. Lacombe, L. Guillemot, V.A. Esaulov, Electron capture and loss processes in the interaction of hydrogen, oxygen, and fluorine atoms and negative ions with a MgO(100) surface, Phys. Rev. Lett. 79 (1997) 3526–3529.